

Electronic Supplementary Information

Microfluidic Synthesis of High-Valence Programmable Atom-Like Nanoparticles for Reliable Sensing

*Jing Li,^{‡a} Huayi Shi,^{‡a} Runzhi Chen,^{‡a} Xiaofeng Wu,^b Jiayi Cheng,^a Fenglin Dong,^{*b} Houyu Wang^{*a} and Yao He^{*a}*

^aLaboratory of Nanoscale Biochemical Analysis, Institute of Functional Nano & Soft Materials (FUNSOM), Soochow University, Soochow University, Suzhou, 215123 (China). E-mail: houyuwang@suda.edu.cn; yaohe@suda.edu.cn

^bDepartment of Ultrasound, The First Affiliated Hospital of Soochow University, Suzhou, 215006 (China). E-mail: fldong@suda.edu.cn

[‡]These authors contributed equally to this work

Table of Contents

1. Reagents and apparatus	S3
2. DNA sequences	S4
3. Experimental procedures	S5
4. Optimization of experimental parameters in the synthesis of cAgNPs	S6
5. Characterization of Au NPs	S8
6. UV-vis spectra of PANs	S9
7. Assignments of Raman spectra	S10
8. COMSOL simulation	S11
9. Finite-difference time domain (FDTD) simulation	S13
10. Calculation of limit of detection (LOD)	S14
11. Comparison of recently reported TET sensors	S15
12. Comparison of SERS enhancement effect in different SERS substrate	S16
13. Kinetics of SSEs adsorption on cAgNPs	S17
14. Selectivity of the developed TET sensor	S18
15. Comparison of TET detection by bulk and microfluidic system	S19
16. References	S20

1. Reagents and apparatus

P-type silicon wafers were bought from Hefei Kejing Materials Technology Co., Ltd. (China). Silver nitrate (AgNO_3 , $\geq 99.8\%$), gold chloride (HAuCl_4 , $\geq 47.8\%$), hydrofluoric acid (HF , $\geq 40\%$), hydrogen peroxide (H_2O_2 , $\geq 30\%$), trisodium citrate ($\geq 99.0\%$) were purchased from Sinopharm Chemical Reagent Co., Ltd. (Shanghai, China). Tetracycline (TET), doxycycline (DOX), oxytetracycline (OTC), Chloramphenicol (CHL) and Vancomycin (VA) were purchased from 3A Chemicals (Shanghai, China). DNA sequences were purchased from Sangon Biotechnology (Shanghai, China). The detailed sequences are listed in Table S1.

The characterizations of the SERS substrate were conducted by a scanning electron microscopy (SEM) (FEI Quanta 200F) equipped with an energy-dispersive X-ray (EDX) spectroscopy (FEI Quanta 200F). The UV-vis spectra were recorded by an UV-vis-near-infrared spectrophotometer (PerkinElmer Lambda 750). Raman spectra were acquired by a Raman microscope (HR800, Horiba Jobin Yvon, France) equipped with a He–Ne laser (633 nm, 0.2 mW, polarized 500:1) and a $100\times$ objective (NA: 0.9). The obtained Raman spectra were further analyzed by the LabSpec5 software. The home-made microfluidic system was equipped with a syringe pump (WH-SP-01, Wenhao Co., Ltd.).

2. DNA sequences

Table S1. DNA sequences utilized in experiments.

name	Sequence (5'-3')
polyA15-p1	AAAAAAAAAAAAAAAAATTTTTCCACAAAATGATTCTGAATTAGCTGT ATC
polyA30-p1	AAAAAAAAAAAAAAAAAAAAAAAAAAAAAAAAATTTTTCCACAAAATG ATTCTGAATTAGCTGTATC
polyA60-p1	AA AAAAAAAAAAAAAAAAATTTTTCCACAAAATGATTCTGAATTAGCTGT ATC
polyA30-p2	AAAAAAAAAAAAAAAAAAAAAAAAAAAAAAAAATTTTTGATACAGCTAA TTCAGAATCATTTTGTGGA
TET aptamer	CGTACGGAATTCGCTAGCCCCCGGCAGGCCACGGCTTGGGTGGTC CCACTGCGCGTGGATCCGAGCTCCACGTG-Cy3 HS-C6-
cDNA	CACGTGGAGCTCGGATCCACGCGCAGTGGGACCAACCCAAGCCGTGG CCTGCCGGGGGGCTAGCGAATTCCGTACG

3. Experimental procedures

Synthesis of AuNPs. Homogeneous AuNPs with the average size of ~10 nm were synthesized by the established citrate reduction method, in which HAuCl₄ solution (0.01%, w/v) is reduced by trisodium citrate solution (1%, w/v) for 20 min at 100 °C.

Kinetics analysis of SSEs adsorption on cAgNPs. Prepare standard solution of Cy5 labeled SSEs (polyA 15/30/60-P1-Cy5) with different concentration (0.4 μM, 0.3 μM, 0.2 μM, 0.15 μM, 0.1 μM, 0.05 μM, 0.25 μM) and record the UV absorbance of Cy5 at 645 nm. To investigate the kinetics of SSEs adsorption on cAgNPs, cAgNPs fabricated in bulk system are incubated with 70 μl sodium phosphate buffer (10 mM, pH=7.0) containing 300 nM SSEs (polyA 15/30/60-P1-Cy5) at 25 °C for 12 h. And 7.77 μl NaCl solution (1M) is added 5 times, finally the concentration of NaCl is 0.1M. Meanwhile, take reaction solution to measure the UV absorbance of unconnected SSEs at different time (0h, 0.5h, 1h, 2h, 4h, 6h, 8h, 10h, 12h). To compare the kinetics of SSEs adsorption on cAgNPs in μ-GD and bulk system, the same solution as above is pumped into the input port with a flow rate of 0.5 μL/min for 8-12 h, and reaction solution at different time point are taken to measure UV absorbance.

4. Optimization of experimental parameters in the synthesis of cAgNPs

As shown in Figure S1a and 1b, mean diameter of cAgNPs increases with the reaction time. Typically, the minimum diameter is 34 nm at 1 min and it goes up to 130 nm at 10 min. As the reaction time prolongs, diameter of particle becomes larger and the gap between particles becomes smaller. When the reaction time is more than 4 min, some particles connect to each other and show irregular morphology. Similarly, as shown in Figure S1c and S1d, the size of cAgNPs also shows AgNO_3 concentration-dependent manner. When the AgNO_3 concentration is more than 0.75 mM, some particles connect to each other and the morphology of some particles becomes irregular. As shown in Figure S1e and S1f, the size of cAgNPs also shows AgNO_3 flow rate-dependent manner. When the AgNO_3 flow rate is more than 3 $\mu\text{L}/\text{min}$, some particles connect to each other and the morphology of some particles becomes irregular.

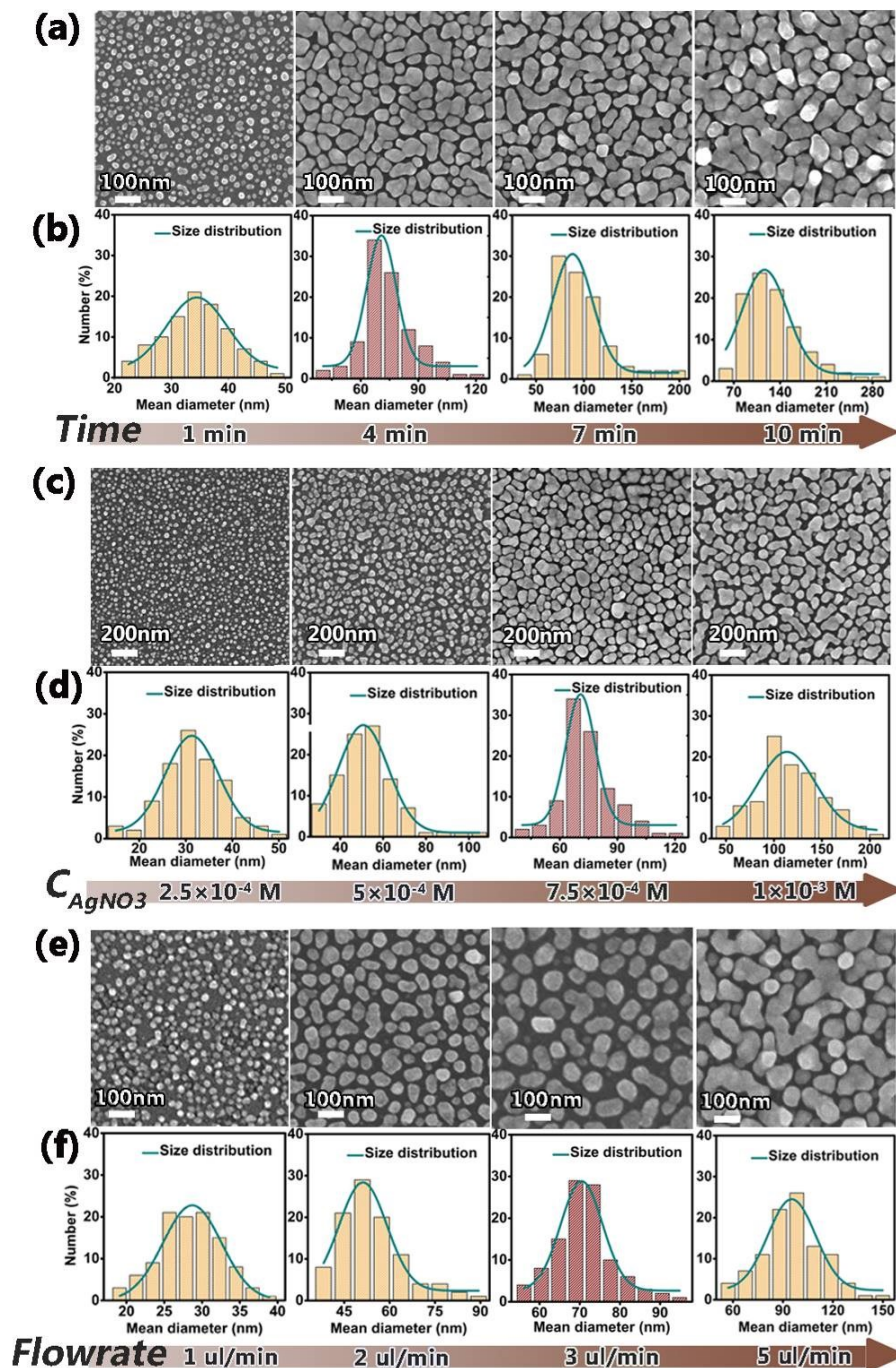


Figure S1. The effects of experimental conditions on the growth of core AgNPs (cAgNPs). (a) SEM images of cAgNPs at different reaction time points and corresponding (b) size distribution. (c) SEM images of cAgNPs at different AgNO_3 concentrations and corresponding (d) size distribution. (e) SEM images of cAgNPs at different AgNO_3 flow rates and corresponding (f) size distribution

5. Characterization of Au NPs

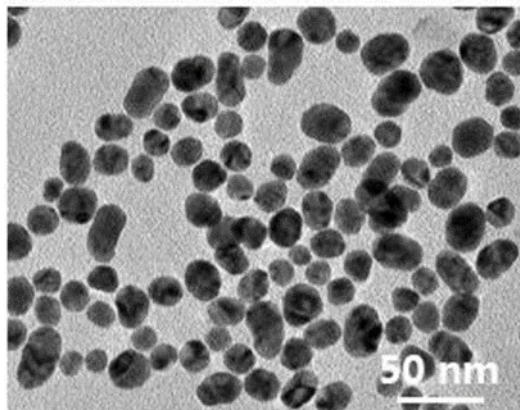


Figure S2. TEM image of the AuNPs

Figure S2 shows the TEM image of the prepared AuNPs with uniform spherical shapes, which are well dispersed in the aqueous phase.

6. UV-vis spectra of PANs.

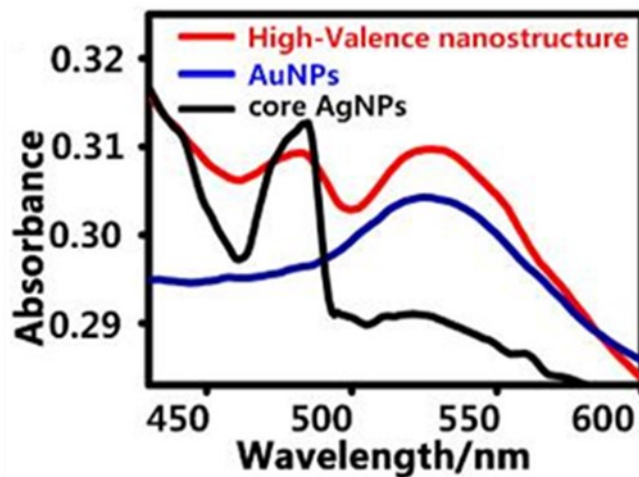


Figure S3. UV-vis spectra of PANs, AuNPs and core AgNPs.

As shown in UV-vis spectra in Figure S3, there are two strong absorption peaks at 473 and 521 nm in the UV-vis spectrum of PANs (red curve), which are respectively assigned to core AgNPs and AuNPs, further confirming the conjugation of AuNPs onto the surface of core AgNPs.

7. Assignments of Raman spectra

Table S2. DNA sequences utilized in experiments.

Vibrational assignment	Observed (cm ⁻¹)	Reported (cm ⁻¹) ^[1]
G	620	621
A, ring breathing	730	730
T,C, ring breathing	787	787
A,G (mainly A)	1327	1325
G and A, $\nu(\text{C}=\text{N})$ imidazole ring(mainly G)	1475	1487
Base ring modes (mainly G and A)	1570	1577
T and C (mainly T), $\nu(\text{C}=\text{O})$	1640	1653

Table S3. Assignments and Raman Shifts (cm-1) for PANs-based TET sensors.

Vibrational assignment	Observed (cm ⁻¹)	Reported (cm ⁻¹) ^[1,2]
G	620	621
A, ring breathing	730	730
T,C, ring breathing	787	787
A,G (mainly A)	1327	1325
$\nu(\text{C}=\text{N})$ stretch of Cy3	1390	1391
$\nu(\text{C}=\text{C})$ ring-stretch of Cy3	1465	1465
G and A, $\nu(\text{C}=\text{N})$ imidazole ring(mainly G)	1475	1487
Base ring modes (mainly G and A)	1570	1577
$\nu(\text{C}=\text{N})$ stretch of Cy3	1586	1586
T and C (mainly T), $\nu(\text{C}=\text{O})$	1640	1653

8. COMSOL simulation

To study the ions and DNA strands distribution, simulation of transportation is performed by using COMSOL Multiphysics (Figure 2e, 2f, 3e and 3f). Concentration of silver ions is set as 7.5×10^{-4} M, and concentration of SSEs (polyA-P1) is set as 300 nM. For pure free diffusion situation, flow velocity is set as 0 μ l/min; for microfluidic system, flow velocity is 3 μ l/min for silver ions and 0.5 μ l/min for SSEs.

In the constructed model, the size of microchannel is set as $200 \times 100 \mu\text{m}$ (equivalent diameter is 1.34×10^{-4} m), the concentration of silver ions (Ag^+) from the inlet is set as 7.5×10^{-4} M and the simulation panel is set as 0.01 mm above silicon support. As for pure diffusion system (flow velocity: 0), the Ag^+ / SSEs transportation across the microchamber is the process of Ag^+ / SSEs diffusion from Ag^+ / SSEs-abundant zone to Ag^+ / SSEs-rare zone. It is assumed that the effect of hydrofluoric acid or buffer on the system is negligible. The mass-balance equation based on Fick's law can be used to describe such diffusive transport:

$$-\nabla(-D\nabla + cu) = 0 \quad (1)$$

where D is the diffusion coefficient of Ag^+ /SSEs in water (m^2/s), c is the Ag^+ /SSEs concentration (mol/m^3), and u is the local velocity (m/s).

As shown in the simulation results of pure diffusion system (Fig. 2f and 3f), Ag^+ /SSEs diffuse slowly and thus an apparent concentration gradient of Ag^+ /SSEs appears in the simulation panel even the simulating time is up to 120 sec for Ag^+ and 200 sec for SSEs.

When the flow velocity is 3 μ l/min for Ag^+ and 0.5 μ l/min for SSEs, the Ag^+ /SSEs transportation in the microfluidic system is the coupled process of creeping flowing and mass diffusion. In such case, the Re is significantly less than 1, the Creeping Flow interface can be used. The convective term in the Navier-Stokes equations can be dropped, leaving the incompressible Stokes equations:

$$\nabla(-pI + \mu(\nabla u + (\nabla u)^T)) = 0 \quad (2)$$

$$\nabla u = 0 \quad (3)$$

where u is the local velocity (m/s) and p is the pressure (Pa).

Therefore, the simulation of Ag^+ /SSEs transfer in microfluidic system is achieved by combining incompressible Stokes equations (Equations 2 and 3) with mass-balance equation (Equation 1). As shown in (Fig. 2e and 3e, homogeneous Ag^+ /SSEs distribution can be quickly reached with

less than 10 sec.

9. Finite-difference time domain (FDTD) simulation

The simulations were carried out using the commercial FDTD software package Lumerical® FDTD Solutions 8.5. Complex electric permittivity of the silicon, silver and gold were adapted from the literatures.^{3,4} Cross section views of simulation region from XY or XZ plane are shown in Figure 4. The diameter of Ag NP is set as 71 nm, and the diameter of Au NP is set as 10 nm. The number of AuNPs for per AgNP is set as 11, and the interparticle distance between Ag NP and Au NP is set as 10 nm for PAN structure and 0 nm for AuNPs-AgNPs@Si (no DNA). The simulation volume is 1 μm (x) by 1 μm (y) by 1 μm (z) with perfectly matched layer boundaries along the x-, y- and z- axes. A plane wave of 633 nm propagating along the $-z$ direction is used as the excitation source, and the polarization of the laser is along $-x$ direction..

10. Calculation of limit of detection (LOD)

The standard curve of TET was given as:

$$Y = A + B \times \text{Log}_{10} X \quad (4)$$

Where A and B are the variable obtained via least-square root linear regression for the signal-concentration curve and variable Y represents the normalized ratiometric SERS signal ($I_{\text{TET}} / I_{\text{BG}}$) at TET concentration of X (C_{TET}).

$$Y = Y_{\text{blank}} + 3SD \quad (5)$$

where SD is the standard deviation and Y blank is the SERS signal of the blank sample. The LOD is calculated as

$$\text{LOD} = 10^{[(Y_{\text{blank}} + 3SD) / Y_{\text{blank}} - A] / B} \quad (6)$$

SD is calculated according to the well-known formula:

$$SD = \sqrt{\frac{1}{n-1} \times \sum_i^n (X_i - X_{\text{average}})^2} \quad (7)$$

where n is the total number of the TET standard sample. X_i is the "i" sample of the series of measurements. X_{average} is the average value of the ratiometric SERS signals obtained from the specific series of identical samples repeated n times. As such, inserting SERS signals into corresponding equations, LOD is calculated as 4.0 fM for the developed TET sensor.

11. Comparison of recently reported TET sensors

Table S4. Comparison of recently reported TET sensors

Method	Limit of detection (nM)	Linear range (μM)	Reference
Fluorescence	20	0.1 -- 60	5
Fluorescence	65.25	0.1125 -- 225	6
Electrochemical	0.05	1.5×10^{-4} -- 6	7
Colorimetric	71	0.1 -- 5	8
Luminescence	225	11.25 -- 56.25	9
This work	4×10^{-6}	1.125×10^{-7} -- 1.125	-

12. Comparison of SERS enhancement effect in different SERS substrate

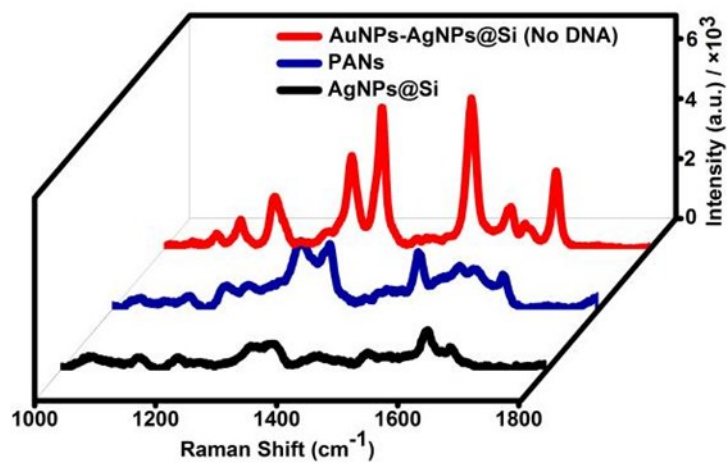


Figure S4. Raman spectra of R6G on the surface of Ag NPs@Si (black), PANs (blue), and AuNPs-AgNPs@Si (black).

13. Kinetics of SSEs adsorption on cAgNPs

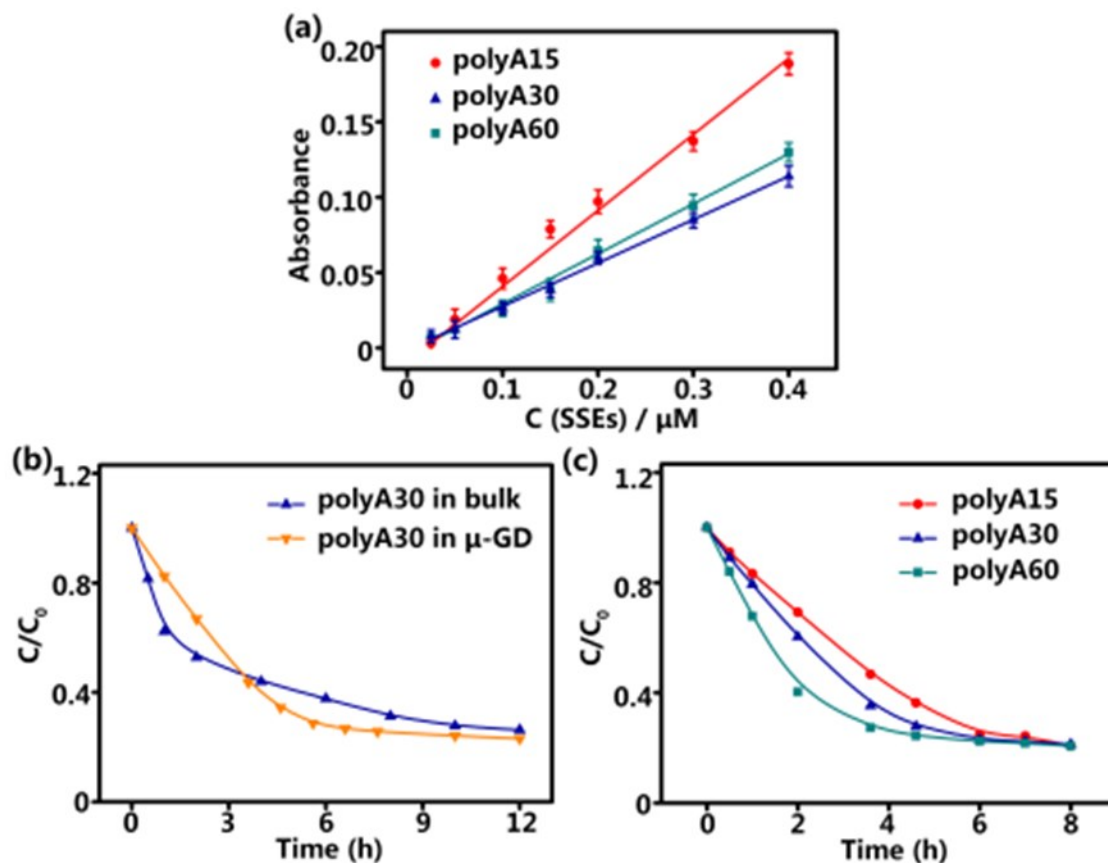


Figure S5. The kinetics of SSEs adsorption on cAgNPs. (a) Linear fitting curves of UV absorbance of Cy5 and concentration of Cy5 labeled SSEs (polyA 15/30/60-P1-Cy5). (b) The kinetic curves of polyA30-P1-Cy5 adsorption on cAgNPs in bulk and microfluidic system. (c) Comparison of kinetics of polyA 15/30/60-P1-Cy5 adsorption onto surface of cAgNPs in microfluidic system.

14. Selectivity of the PANs-based sensors

To evaluate the selectivity of PANs-based sensors, Raman spectra are collected by parallel measurements of four kinds of interfering antibiotics (e.g., doxycycline (DOX), oxytetracycline (OTC), chloramphenicol (CHL) and vancomycin (VA)) at the concentration of 1125 nM. As shown in Figure S6a and 6b, strong SERS spectra and ratiometric signals of I_{1586}/I_{730} are only found in TET group while much weaker ratiometric signals are observed in other four interfering groups and blank control group, verifying the good selectivity of the developed sensors for discriminating TET against other interfering antibiotics.

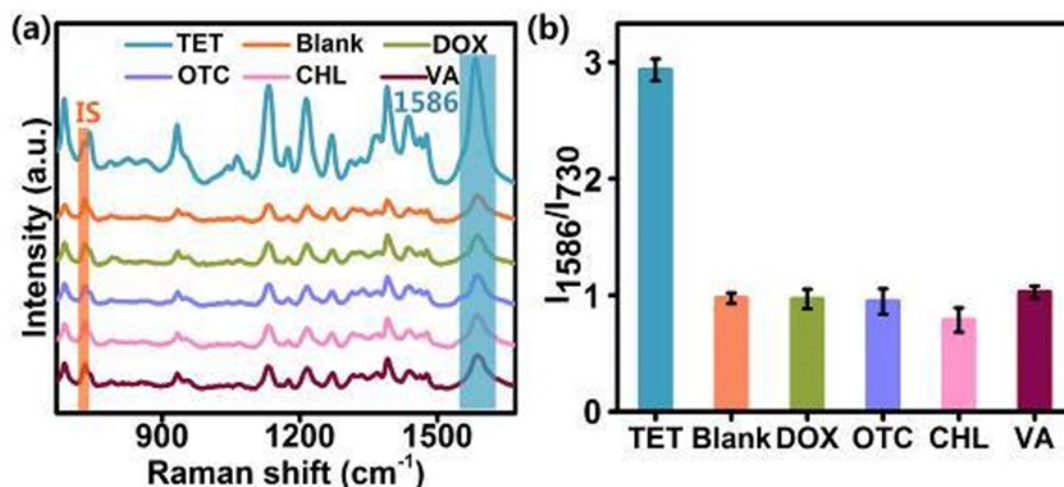


Figure S6. (a) Raman spectra and (b) corresponding ratiometric signals of I_{1586}/I_{730} from the developed PANs-based sensors in the presence of various kinds of antibiotics (DOX, OTC, CHL and VA, 1125 nM for each sample)

15. Comparison of TET detection by bulk and microfluidic system

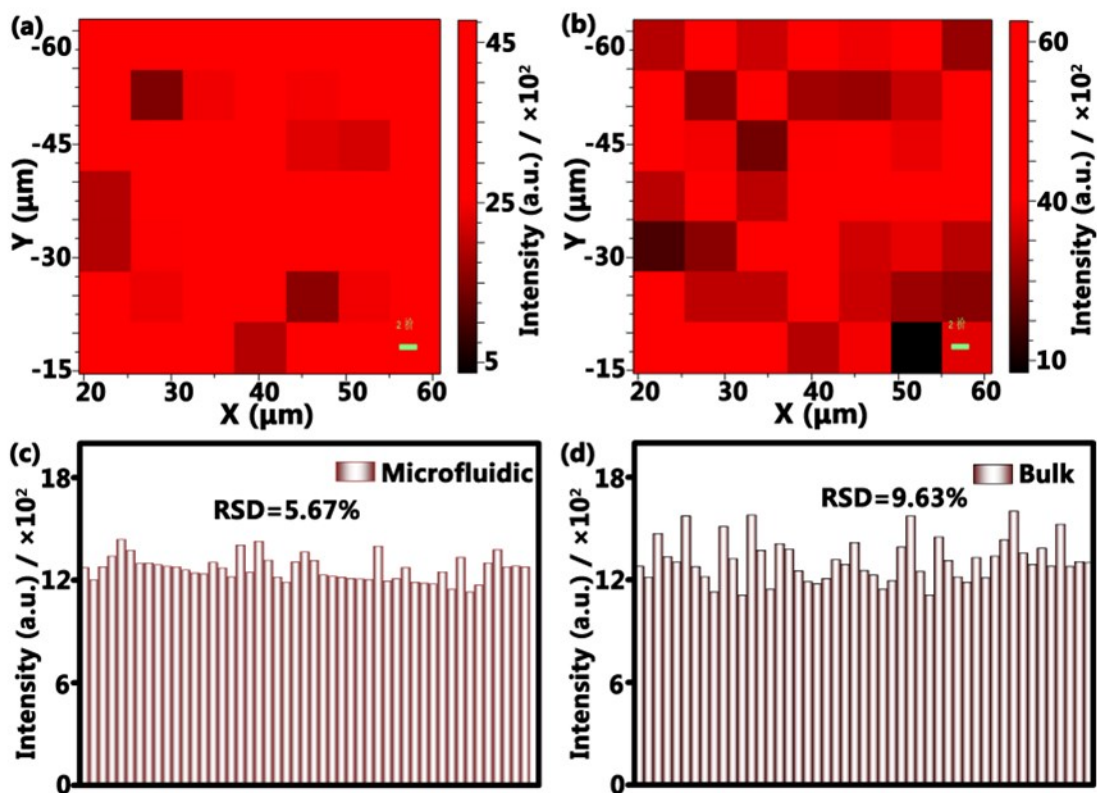


Figure S7. SERS mapping of Cy3 at 1586 cm^{-1} from (a) microfluidic system and (b) bulk system (CTET = 1125 nM). And corresponding Raman intensities at 1586 cm^{-1} from microfluidic (c) and bulk system (d).

16. References

- 1 L. J. Xu, Z. C. Lei, J. Li, C. Zong, C. J. Yang, B. Ren, *J. Am. Chem. Soc.* 2015, **137**, 5149-5154.
- 2 S. Ye, Y. Wu, X. Zhai, B. Tang, *Anal. Chem.* 2015, **87**, 8242-8249..
- 3 E. D. Palik, Elsevier, Amsterdam, 1998.
- 4 P. B. Johnson, R. W. Christy, *Phys. Rev. B* 1972, **6**, 4370–4379..
- 5 H. B. Wang, Y. Li, H. Y. Bai, Z. P. Zhang, Y. H. Li, Y. M. Liu, *Food Anal. Methods.* 2018, **11**, 3095-3102.
- 6 M. Y. Qi, C. Y. Tu, Y. Y. Dai, W. P. Wang, A. J. Wang, J. R. Chen, *Anal. Methods* 2018, **10**, 3402-3407..
- 7 Y. Tang, P. Liu, J. Xu, L. Li, L. Yang, X. Liu, S. Liu, Y. Zhou, *Sensor. Actuat. B-Chem.* 2018, **258**, 906-912.
- 8 C. Yang, J. Bie, X. Zhang, C. Yan, H. Li, M. Zhang, R. Su, X. Zhang, C. Sun, *Spectrochim. Acta. A* 2018, **202**, 382-388.
- 9 C. Sun, R. Su, J. Bie, H. Sun, S. Qiao, X. Ma, R. Sun, T. Zhang, *Dyes Pigm.* 2018, **149**, 867-875.